Scaling of p_T distributions for p and $\bar{p}$ produced in Au+Au collisions at $\sqrt{s_{NN}} = 200$ GeV

W. C. Zhang, Y. Zeng, W. X. Nie, L. L. Zhu, and C. B. Yang
Institute of Particle Physics, Hua-Zhong Normal University, Wuhan 430079, People's Republic of China
(Received 26 April 2007; revised manuscript received 1 August 2007; published 29 October 2007)

With the experimental data from STAR and PHENIX on the centrality dependence of the p_T spectra of protons and antiprotons produced at midrapidity in Au+Au collisions at 200 GeV, we show that for protons and antiprotons there exists a scaling distribution independent of the colliding centrality. The scaling functions can also describe data from BRAHMS for both proton and antiproton spectra at $y = 2.2$ and 3.2. The scaling behaviors are shown to be incompatible with the usual string fragmentation scenario for particle production.

DOI: 10.1103/PhysRevC.76.044910 PACS number(s): 25.75.Dw, 13.85.Ni

I. INTRODUCTION

One of the most important quantities in investigating properties of the medium produced in high energy collisions is the particle distribution for different species of final state particles. RHIC experiments have found a lot of novel phenomena from the particle spectra, such as the unexpectedly large p/π ratio at $p_T \sim 3\text{GeV}/c$ [1], the constituent quark number scaling of the elliptic flows [2], and strong nuclear suppression of the pion spectrum in central Au+Au collisions [3], etc. From the spectrum one can learn a lot on the dynamics for particle production.

In many studies, searching for a scaling behavior of some quantities vs suitable variables is useful for unveiling potential universal dynamics. A typical example is the proposal of the parton model from the x-scaling of the structure functions in deep-inelastic scatterings [4]. Quite recently, a scaling behavior [5] of the pion spectrum at midrapidity in Au+Au collisions at RHIC was found, which related spectra with different collision centralities. In [6] the scaling behavior was extended to noncentral region, up to $\eta = 3.2$ for both Au+Au and d+Au collisions. The same scaling function can be used to describe pion spectra for p_T up to a few GeV/c from different colliding systems at different rapidities and centralities. The shape of pion spectrum in those collisions is determined by only one parameter $\langle p_T \rangle$, the mean transverse momentum of the particle. It is very interesting to ask whether similar scaling behaviors can be found for spectra of other particles produced in Au+Au collisions at RHIC. In this paper, the scaling property of the spectra for protons and antiprotons is investigated and compared with that for pions.

The organization of this paper is as follows. In Sec. II we will address the procedures for searching the scaling behaviors. Then in Sec. III the scaling properties of the spectra for protons and antiprotons produced in Au+Au collisions at RHIC at $\sqrt{s_{NN}} = 200\,\text{GeV}$ will be studied. We discuss mainly the centrality scaling of the spectra at midrapidity and extend the discussion to very forward region with rapidity $y = 2.2$ and 3.2 briefly. Section IV is for discussions on the relation between the scaling behaviors and the string fragmentation scenario.

II. METHOD FOR SEARCHING THE SCALING BEHAVIOR OF THE SPECTRUM

As done in [5,6], the scaling behavior of a set of spectra at different centralities can be searched in a few steps. First, we define a scaled variable

$$z = p_T/K, \tag{1}$$

and the scaled spectrum

$$\Phi(z) = A \left. \frac{d^2N}{2\pi p_T dp_T dy} \right|_{p_T = Kz}, \tag{2}$$

with K and A free parameters. As a convention, we choose $K = A = 1$ for the most central collisions. With this choice $\Phi(z)$ is nothing but the p_T distribution for the most central collisions. For the spectra with other centralities, we try to coalesce all data points to one curve by choosing proper parameters A and K. If this can be achieved, a scaling behavior is found. The detailed expression of the scaling function depends, of course, on the choice of A and K for the most central collisions. This arbitrary can be overcome by introducing another scaling variable

$$u = z/\langle z \rangle = p_T/\langle p_T \rangle, \tag{3}$$

and the normalized scaling function

$$\Psi(u) = \langle z \rangle^2 \Phi(\langle z \rangle u) \Big/ \int_0^\infty \Phi(z) z\, dz. \tag{4}$$

Here $\langle z \rangle$ is defined as

$$\langle z \rangle \equiv \int_0^\infty z\Phi(z) z dz \Big/ \int_0^\infty \Phi(z) z dz. \tag{5}$$

By definition, $\int_0^\infty \Psi(u) u du = \int_0^\infty u\Psi(u) u du = 1$. This scaled transverse momentum distribution is in essence similar to the KNO-scaling [7] on multiplicity distribution.

III. SCALING BEHAVIORS OF PROTON AND ANTI-PROTON DISTRIBUTIONS

Now we focus on the spectra of protons and antiprotons produced at midrapidity in Au+Au collisions at

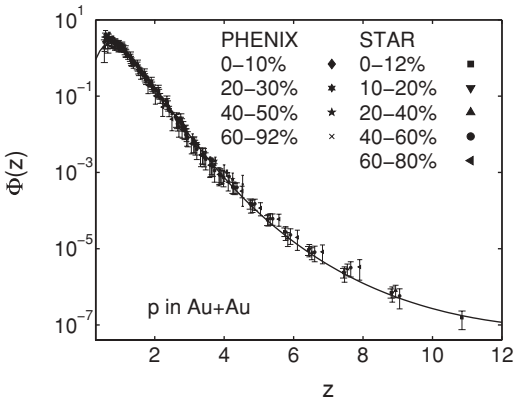

FIG. 1. Scaling behavior of the spectrum for protons produced at midrapidity in Au+Au collisions at RHIC. The data are taken from [8,9]. Feed-down corrections are considered in the data. The solid curve is from Eq. (6).

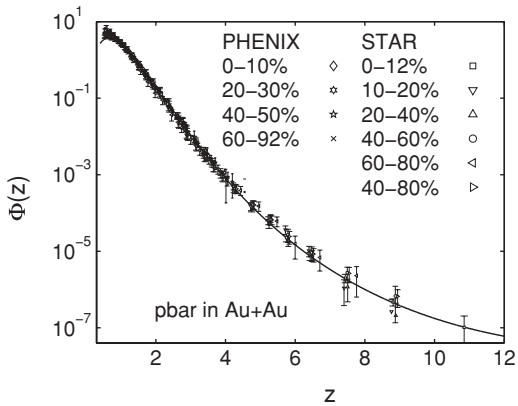

FIG. 2. Scaling behavior of the spectrum for antiprotons produced at midrapidity in Au+Au collisions at RHIC. The data are taken from [8,9]. Feed-down effects are not corrected in the STAR data for $\bar{p}$. The solid curve is from Eq. (7).

$\sqrt{s_{NN}} = 200\,\text{GeV}$. STAR and PHENIX Collaborations at RHIC published spectra for protons and antiprotons at midrapidity for a set of colliding centralities [8,9]. STAR data have a p_T coverage larger than PHENIX ones. As shown in Fig. 1, all data points for proton spectra at different centralities can be put to the same curve with suitably chosen A and K, by the procedure explained in last section. The parameters are shown in Table I. Except a few points for very peripheral collisions (centralities 60–92% for PHENIX data and 60–80% for STAR data), all points agree well with the curve in about six orders of magnitude. The larger deviation of data at centralities 60–92% for PHENIX and 60–80% for STAR from the scaling curve may be due to the larger centrality coverage, because the size of colliding system changes dramatically in those centrality bins. For simplicity we define $v = \ln(1+z)$, and the curve can be parametrized as

$$\Phi_p(z) = 0.052 \exp\left(14.9v - 16.2v^2 + 3.3v^3\right). \tag{6}$$

Similarly, one can put all data points for antiproton spectra at different centralities to a curve with other sets of parameters A and K which are given also in Table I. The agreement is good, as can be seen from Fig. 2, with only a few points in small p_T region for peripheral collisions departing a little from the curve. For antiproton the scaling function is

$$\Phi_{\bar{p}}(z) = 0.16 \exp\left(13v - 14.9v^2 + 2.9v^3\right), \tag{7}$$

with v defined above.

To see how good is the agreement between the fitted curves in Figs. 1 and 2 and the experimental data, one can calculate a ratio

$$B = \text{experimental data/fitted results},$$

and show B as a function of p_T in linear scale for all the data sets, as shown in Fig. 3 for the case of the proton. From

TABLE I. Parameters for coalescing all data points to the same curves in Figs. 1 and 2.

STAR centrality	p		$\bar{p}$	
	K	A	K	A
0–12%	1	1	1	1
10–20%	0.997	1.203	1.005	1.417
20–40%	0.986	2.009	0.991	2.305
40–60%	0.973	4.432	0.993	5.414
60–80%	0.941	13.591	0.959	16.686
40–80%			0.986	8.126
PHENIX centrality	p		$\bar{p}$	
	K	A	K	A
0–10%	1.042	1.226	1.068	2.404
20–30%	1.026	2.532	1.045	4.901
40–50%	1.031	6.253	1.013	11.754
60–92%	0.934	39.056	0.935	69.31
BRAHMS centrality	p		$\bar{p}$	
	K	A	K	A
$y = 2.2$			0.930	0.921
$y = 3.2$	1.079	0.754	1.153	6.985

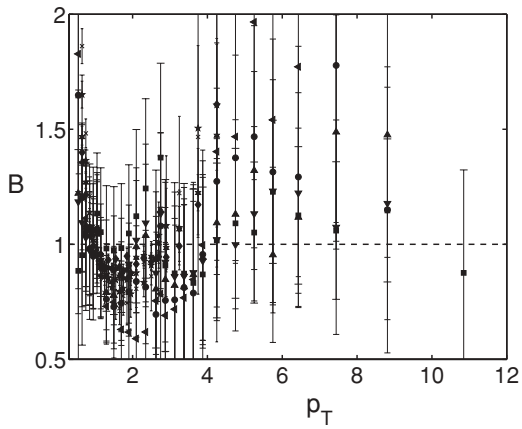

FIG. 3. Ratio between experimental data and the fitted results shown in Fig. 1. STAR and PHENIX data are taken from [8,9]. Symbols are the same as in Fig. 1.

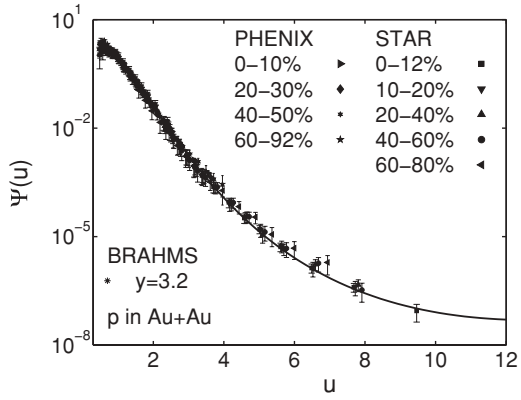

FIG. 4. Normalized scaling distribution for protons produced at midrapidity and very forward direction in Au+Au collisions at RHIC with the scaling variable u. STAR and PHENIX data are taken from [8,9] and BRAHMS data from [10].

the figure one can see that almost all the points have values of B within 0.7 to 1.3, which means that the scaling is true within an accuracy of 30%. This is quite a good fit, considering the fact that the data cover about 6 orders of magnitude. For antiprotons, the agreement is better than for protons.

Now one can see that the transverse momentum distributions for protons and antiprotons satisfy a scaling law. For large p_T (thus large z) the scaling functions in Eqs. (6) and (7) behave as powers of p_T, though the expressions are not in powers of z or p_T. The scaling functions in Eqs. (6) and (7) depend on the choices of A and K for the case with centrality 0–12% for STAR data. With the variable u defined in Eq. (3) this dependence can be circumvented. $\langle z \rangle$'s for protons and antiprotons are 1.14 and 1.08, respectively, with integration over z in the range from 0 to 12, roughly corresponding to the p_T range measured by STAR. The normalized scaling functions $\Psi(u)$ for protons and antiprotons can be obtained easily from Eqs. (6) and (7) and are shown in Figs. 4 and 5, respectively, together with scaled data points as in Figs. 1 and 2. A simple parametrization for the two normalized scaling functions in Figs. 4 and 5 can be given as follows:

$$\Psi_p(u) = 0.064 \exp(13.6v - 16.67v^2 + 3.6v^3),$$
$$\Psi_{\bar{p}}(u) = 0.086 \exp(12.41v - 15.31v^2 + 3.16v^3),$$

with $v = \ln(1 + u)$.

As in the case for pion distributions, one can also investigate the p_T distributions of protons and antiprotons in noncentral rapidity regions in Au+Au collisions. The only data set we can find is from BRAHMS [10] at rapidity $y = 2.2$ and 3.2 with centrality 0–10%. It is found that the BRAHMS data can also be put to the same scaling curves, as shown in Figs. 4 and 5. The values of corresponding parameters A and K are also given in Table I. Thus the scaling distributions found in this paper may be valid in both central and very forward regions for protons and antiprotons produced in Au+Au collisions at RHIC at $\sqrt{s_{NN}} = 200$ GeV.

Now one can ask for the difference between the scaling functions for protons and antiprotons. After normalization to 1 the difference between the scaling distributions $\Psi(u)$ for protons and antiprotons is shown in Fig. 6. In log scale the difference between the two scaling functions is invisible at low u. To show the difference clearly a ratio $r = \Psi_p(u)/\Psi_{\bar{p}}(u)$ is plotted in the inset of Fig. 6 as a function of u. The increase of r with u is in agreement qualitatively with data shown in [9] where it is shown that $\bar{p}/p$ decreases with p_T monotonically. The difference in the two scaling functions can be understood physically. In Au+Au collisions there are much more quarks u, d than $\bar{u}$ and $\bar{d}$ in the initial state. In the central region in the state just before hadronization, more u and d quarks can be found because of the nuclear stopping effect in the interactions. As a consequence, more protons can be formed from the almost thermalized quark medium than antiprotons in the small p_T regime. Experimental data show that in low p_T region the yield of antiproton is about 80% that of protons in central Au+Au collisions at RHIC. This difference contributes to the net baryon density in the central region in Au+Au collisions at RHIC. On the other hand, in the large p_T region, protons and antiprotons are formed mainly from fragmentation of hard partons produced in the QCD interactions with large

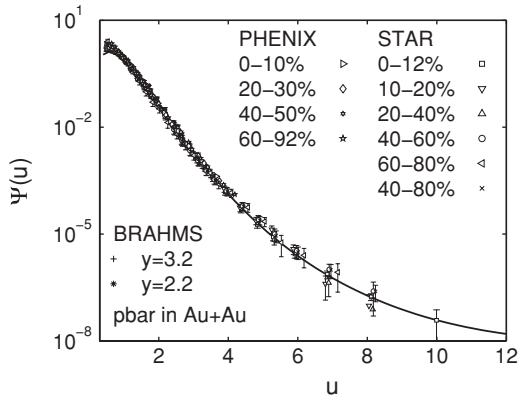

FIG. 5. Normalized scaling distribution for antiprotons produced at midrapidity and very forward direction in Au+Au collisions at RHIC with the scaling variable u. STAR and PHENIX data are taken from [8,9] and BRAHMS data from [10].

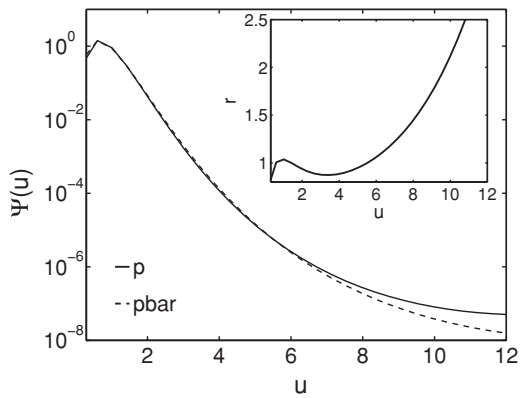

FIG. 6. Comparison between the scaling functions for protons and antiprotons produced at midrapidity in Au+Au collisions at RHIC with the scaling variable u. The inset if for the ratio $\Psi_p(u)/\Psi_{\bar{p}}(u)$.

TABLE II. Ratio of moments $\langle p_T^n \rangle / \langle p_T \rangle^n$ for protons, antiprotons, and pions produced in Au+Au collisions at RHIC.

n	p	$\bar{p}$	π
2	1.194	1.215	1.65
3	1.717	1.775	4.08
4	2.978	3.064	14.4
5	6.415	6.417	64.73
6	19.045	17.253	373.82

momentum transfer. As shown in [11], the gluon yield from hard processes is about five times that of u and d quarks. The fragmentation from a gluon to p and $\bar{p}$ is the same. The amount of u, d quarks from hard processes is about 10 times that of $\bar{u}, \bar{d}$ when the hard parton's transverse momentum is high enough. It is well-known that the fragmentation function for a gluon to p or $\bar{p}$ is much smaller than that for a u or d ($\bar{u}$ or $\bar{d}$) to $p(\bar{p})$ because of the dominant valence quark contribution to the latter process. As a result, the ratio of yields of proton over antiproton at large p_T is even more than that at small p_T. After normalizing the distributions to the scaling functions the yield ratio of proton over anti-proton increases approximately linearly with u when u is large. It should be mentioned that no such difference for π^+, π^-, and π^0, because they all are composed of a quark and an antiquark.

The scaling behaviors of the p_T distribution functions for protons and antiprotons can be tested experimentally from studying the ratio of moments of the momentum distribution, $\langle p_T^n \rangle / \langle p_T \rangle^n = \int_0^\infty u^n \Psi(u) u du$ for $n = 2, 3, 4, \ldots$. From the determined normalized distributions, the ratio can be calculated by integrating over u in the range from 0 to 12, as mentioned above, and the results are tabulated in Table II. The values of the ratio are independent of the parameters A and K in the fitting process but only on the functional form of the scaling distributions. If the scaling behaviors of particle distributions are true, such ratios should be constants independent of the colliding centralities and rapidities. For comparison, the corresponding values of the ratio for pions produced in the same interactions, calculated in [6], are also given in Table II. Because of very small difference in the scaling distributions for protons and antiprotons at small u, the ratio for protons increases with n at about the same rate as for antiproton for small n. For large n, the ratio for p becomes larger than that for $\bar{p}$ because of the big difference in the scaling functions for p and $\bar{p}$ at large u. Because of the very strong suppression of high transverse momentum proton production relative to that of pions, the ratio for pions increases with n much more rapidly than for p and $\bar{p}$.

Another important question is about the difference between the scaling functions for protons in this paper and for pions in [5,6]. Experiments at RHIC have shown that the ratio of proton yield over that of pion increases with p_T up to 1 in the region $p_T \leqslant 3$ GeV/c and saturates in large p_T region. This behavior should be seen from the scaling functions for these two species of particles. For the purpose of comparing the scaling distributions we define a ratio

$$R = \Psi_p(u) / \Psi_\pi(u), \tag{8}$$

and plot the ratio R as a function of u in Fig. 7. The ratio increases with u, when u is small, reaches a maximum at u about 1 and then decreases. Finally it decreases slowly to about 0.1 for very large u. The highest value of R is about 1.6, while the experimentally observed p over π ratio is about 1 at $p_T \sim 3$ GeV/c. The reason for this difference is two-fold.One is the normalization difference in defining R and the experimental ratio. Another lies in the different mean transverse momenta $\langle p_T \rangle$'s for pions and protons with which the scaling variable u is defined and used in getting the ratio R.

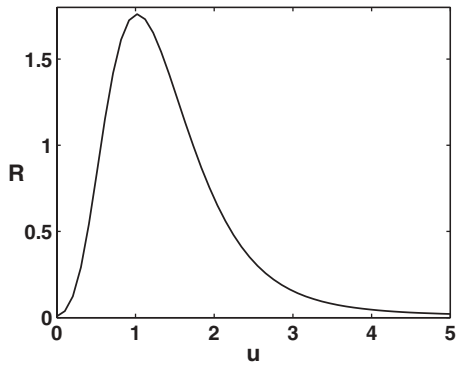

FIG. 7. Ratio $\Psi_p(u)/\Psi_\pi(u)$ between the scaling functions for protons and pions produced in Au+Au collisions at RHIC as a function of the scaling variable u. The pion scaling distribution is from [5,6].

The existence of difference in the scaling distributions for different species of particles produced in high energy collisions is not surprising, because the distributions reflect the particle production dynamics which may be different for different particles. In the quark recombination models [12–14] pions are formed by combining a quark and an antiquark while protons by three quarks. Because different numbers of (anti)quarks participate in forming the particles, their scaling distributions must be different. In this sense, our investigation results urge more studies on particle production mechanisms.

IV. DISCUSSIONS

From the above investigation we have found scaling distributions for protons and antiprotons produced in Au+Au collisions at RHIC in both midrapidity and forward region. The difference between those two scaling distributions is quite small, but they differ a lot from that for pions and the ratio Ψ_p/Ψ_π exhibits a nontrivial behavior.

Investigations in [5,6] and in this paper have shown that particle distributions can be put to the same curve by linear transformation on p_T. Though we have not yet a uniform picture for the particle productions in high energy nuclear collisions, the scaling behaviors can, in some sense, be compared to that from the string fragmentation picture [15]. In that picture if there are n strings, they may overlap in an area of S_n and the average area for a string is then S_n/n. It is shown that the momentum distributions can be related to the

case in pp collisions also by a linear variable change $p_T \rightarrow p_T((S_n/n)_{\mathrm{AuAu}}/(S_n/n)_{pp})^{1/4}$. Viewed from that picture, our fitted K gives the degree of string overlap. The average area for a string in most central Au+Au collisions is about 70% of that in peripheral ones from the values of K obtained from fitting the spectra of proton. If string fragmentation is really the production mechanism for all species of particles in the collisions, one can expect that the overlap degree obtained is the same from the changes of spectrum of any particle. In the language in this work, values of K are expected the same for pions, protons and other particles in the string fragmentation picture for particle production. Our results show the opposite. Comparing the values of K from [5] and this work, one can see that for pion spectrum K is larger for more peripheral collisions but smaller for proton and antiproton spectra. Our results indicate that other particle production mechanisms may also provide ways to the scaling distributions. Obviously more detailed studies, both theoretically and experimentally, are needed.

ACKNOWLEDGMENTS

This work was supported in part by the National Natural Science Foundation of China under Grant Nos. 10635020 and 10475032, by the Ministry of Education of China under Grant No. 306022 and project IRT0624.

[1] S. S. Adler *et al*. (PHENIX Collaboration), Phys. Rev. C **69**, 034909 (2004).
[2] D. Molnár and A. Voloshin, Phys. Rev. Lett. **91**, 092301 (2003); P. Sorensen (STAR Collaboration), J. Phys. G **30**, S217 (2004).
[3] See, for example, S. S. Adler (PHENIX Collaboration), Phys. Rev. Lett. **91**, 072301 (2003).
[4] J. D. Bjorken and E. A. Paschos, Phys. Rev. **185**, 1975 (1969).
[5] R. C. Hwa and C. B. Yang, Phys. Rev. Lett. **90**, 212301 (2003).
[6] L. L. Zhu and C. B. Yang, Phys. Rev. C **75**, 044904 (2007).
[7] Z. Koba, H. B. Nielsen, and P. Olesen, Nucl. Phys. **B40**, 317 (1972).
[8] S. S. Adler *et al*. (PHENIX Collaboration), Phys. Rev. Lett. **91**, 172301 (2003).
[9] B. I. Abelev *et al*. (STAR Collaboration), Phys. Rev. Lett. **97**, 152301 (2006).
[10] R. Karabowicz for the BRAHMS Collaboration, talk at Quark Matter 2005, Budapest, Hungary [Nucl. Phys. **A774**, 447 (2006)]; I. Arsene *et al*. (BRAHMS Collaboration), nucl-ex/0610021.
[11] D. K. Srivastava, C. Gale, and R. J. Fries, Phys. Rev. C **67**, 034903 (2003).
[12] R. C. Hwa and C. B. Yang, Phys. Rev. C **67**, 034902 (2003).
[13] V. Greco, C. M. Ko, and P. Lévai, Phys. Rev. Lett. **90**, 202302 (2003); Phys. Rev. C **68**, 034904 (2003).
[14] R. J. Fries, B. Müller, C. Nonaka, and A. Bass, Phys. Rev. Lett. **90**, 202303 (2003); Phys. Rev. C **68**, 044902 (2003).
[15] M. A. Braun, F. del Moral, and C. Pajares, Nucl. Phys. **A715**, 791 (2003).